Inorganic Chemistry

pubs.acs.org/IC Article

Synthesis, Characterization, and Biological Activity of Water-Soluble, Dual Anionic and Cationic Ruthenium–Arene Complexes Bearing Imidazol(in)ium-2-dithiocarboxylate Ligands

Mohammed Zain Aldin, Guillermo Zaragoza, William Deschamps, Jean-Claude Didelot Tomani, Jacob Souopgui, and Lionel Delaude*

Cite This: *Inorg. Chem.* 2021, 60, 16769–16781 Read Online

ACCESS | Metrics & More | Article Recommendations | Supporting Information

ABSTRACT: An efficient synthetic protocol was devised for the preparation of five cationic ruthenium–arene complexes bearing imidazol(in)ium-2-dithiocarboxylate ligands from the $[RuCl_2(p\text{-cymene})]_2$ dimer and *2 equiv* of an NHC·CS_2 zwitterion. The reactions proceeded cleanly and swiftly in dichloromethane at room temperature to afford the expected $[RuCl(p\text{-cymene})(S_2C{\cdot}NHC)]Cl$ products in quantitative yields. When the $[RuCl_2(p\text{-cymene})]_2$ dimer was reacted with only *1 equiv* of a dithiolate betaine under the same experimental conditions, a set of five bimetallic compounds with the generic formula $[RuCl(p\text{-cymene})(S_2C{\cdot}NHC)][RuCl_3(p\text{-cymene})]$ was obtained in quantitative yields. These novel, dual anionic and cationic ruthenium–arene complexes were fully characterized by various analytical techniques. NMR titrations showed that the chelation of the dithiocarboxylate ligands to afford $[RuCl(p\text{-cymene})(S_2C{\cdot}NHC)]^+$ cations was quantitative and irreversible. Conversely, the formation of the $[RuCl_3(p\text{-cymene})]^-$ anion was limited by an equilibrium, and this species readily dissociated into Cl^- anions and the $[RuCl_2(p\text{-cymene})]_2$ dimer. The position of the equilibrium was strongly influenced by the nature of the solvent and was rather insensitive to the temperature. Two monometallic and two bimetallic complexes cocrystallized with water, and their molecular structures were solved by X-ray diffraction analysis. Crystallography revealed the existence of strong interactions between the azolium ring protons of the cationic complexes and neighboring donor groups from the anions or the solvent. The various compounds under investigation were highly soluble in water. They were all strongly cytotoxic against K562 cancer cells. Furthermore, with a selectivity index of 32.1, the $[RuCl(p\text{-cymene})(S_2C{\cdot}SIDip)]Cl$ complex remarkably targeted the erythroleukemic cells vs mouse splenocytes.

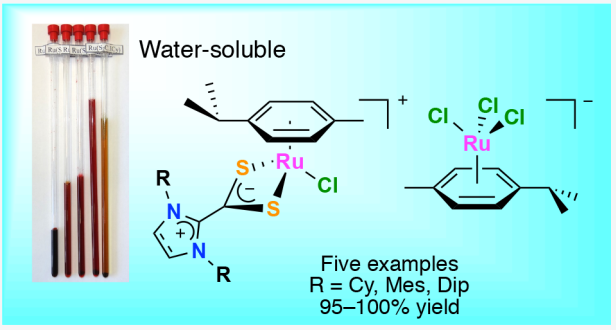

INTRODUCTION

N-Heterocyclic carbenes (NHCs) are powerful nucleophiles that react instantaneously with carbon disulfide to afford stable zwitterions conveniently designated as NHC·CS_2 adducts.[1,2] These inner salts are usually crystalline materials that form strong M–S bonds with a wide range of metal centers.[3] Borer and co-workers first investigated their coordination chemistry in the 1980s by synthesizing various complexes from 1,3-dimethylimidazolium-2-dithiocarboxylate (IMe·CS_2) and diverse late transition metal halides or nitrates.[4] The products obtained were characterized by IR and UV/visible spectroscopies. Cyclic voltammetry, electrical conductivity, and magnetic susceptibility measurements were performed in some instances; but no NMR or XRD data were provided, and the molecular structures proposed remained hypothetical.

In 2009, while investigating the ability of NHC·CO_2 and NHC·CS_2 zwitterions to generate *in situ* ruthenium–NHC catalyst precursors for olefin metathesis and atom transfer radical polymerization reactions, we synthesized and fully characterized the first representatives of well-defined organometallic species featuring imidazolium or imidazolinium-2-dithiocarboxylate ligands.[5] Thus, five cationic ruthenium–arene complexes featuring κ^2-*S*,*S*′ chelates (**1a**–**e**) were isolated in high yields upon reaction of the $[RuCl_2(p\text{-cymene})]_2$ dimer (*p*-cymene is 1-isopropyl-4-methylbenzene) with 2 equiv of an NHC·CS_2 zwitterion and potassium hexafluorophosphate in ethanol at 60 °C for 1 h (Scheme 1).

Subsequent investigations carried out in collaboration with the group of Wilton-Ely at Imperial College allowed the extension of the coordination chemistry of the 1,1-dithiolate betaines to other sources of ruthenium,[6,7] as well as osmium,[7] palladium,[8] and gold.[9] In 2016–2017, we described the

Received: August 26, 2021
Published: October 20, 2021

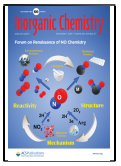

https://doi.org/10.1021/acs.inorgchem.1c02648
Inorg. Chem. 2021, 60, 16769–16781

Scheme 1. Synthesis of Cationic Ruthenium−Arene Complexes Bearing Imidazol(in)ium-2-dithiocarboxylate Ligands

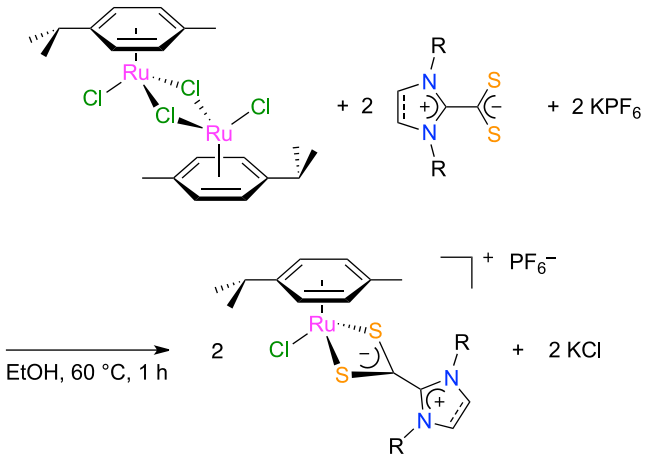

1a: NHC = IMes (75%)
1b: NHC = IDip (69%)
1c: NHC = ICy (80%)
1d: NHC = SIMes (69%)
1e: NHC = SIDip (89%)

formation of mono- and bimetallic metal−carbonyl compounds based on manganese[10] and rhenium[11] that featured chelating or bridging NHC·CS_2 ligands.[12] More recently, we disclosed the synthesis of superbulky imidazolium-2-dithiocarboxylate ligands and their complexation to rhenium and ruthenium,[13] while other researchers relied on NHC·CS_2 betaines to prepare copper-based coordination polymers[14] and clusters[15] or gold nanoparticles[9] and self-assembled monolayers.[16] A few reports on the formation of dinuclear iron−carbonyl[17] and tetranuclear ruthenium−carbonyl clusters,[18] in which the dithiocarboxylate unit underwent chemical transformations, also appeared in the literature.

In light of our sustained interest in ruthenium−arene catalyst precursors[19] and azolium-2-dithiocarboxylate betaines,[3] we decided to reassess our 2009 study[5] and to delve further into the reactivity of the $[RuCl_2(p\text{-cymene})]_2$ dimer with NHC·CS_2 zwitterions. Herein, we disclose a new efficient synthetic protocol for the preparation of monometallic [RuCl(*p*-cymene)(S_2C·NHC)]Cl complexes. We also investigate the influence of the Ru/dithiolate ligand ratio on the outcome of the reaction, and we show that a 1:1 mixture of the metal dimer and five different NHC·CS_2 zwitterions cleanly and transiently affords dual anionic and cationic [RuCl(*p*-cymene)(S_2C·NHC)][$RuCl_3$(*p*-cymene)] complexes, which are remarkably water-soluble and biologically active against tumorous cells.

RESULTS AND DISCUSSION

Synthesis of Monometallic [RuCl(*p*-cymene)(S_2C·NHC)]Cl Complexes. The five representative NHC·CS_2 zwitterions that we selected in 2009 were employed again in the present work.[5] They include three unsaturated imidazolium-dithiocarboxylate inner salts bearing aliphatic or aromatic substituents of increasing bulkiness on their nitrogen atoms, namely, the cyclohexyl (Cy), mesityl (Mes), and 2,6-diisopropylphenyl (Dip) groups, together with two imidazolinium derivatives nicknamed SIMes·CS_2 and SIDip·CS_2 (Chart 1).

Chart 1. Imidazol(in)ium-2-dithiocarboxylate Ligands Used in This Work

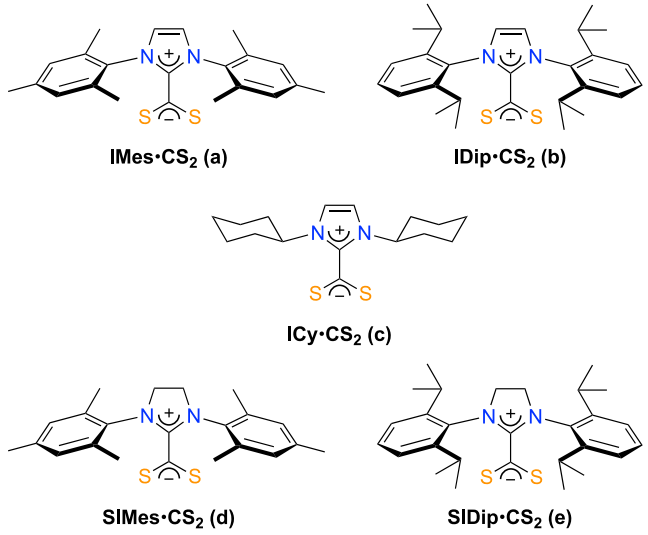

IMes·CS_2 (a) IDip·CS_2 (b)
ICy·CS_2 (c)
SIMes·CS_2 (d) SIDip·CS_2 (e)

Preliminary experiments were carried out in NMR tubes charged with the $[RuCl_2(p\text{-cymene})]_2$ dimer (20 mg) and 2 equiv of an NHC·CS_2 zwitterion. Upon the addition of $CDCl_3$ (0.5 mL) and slowly mixing, a homogeneous solution was obtained, whose color quickly changed from orange-red to dark red-purple. After 10 min at room temperature, ^{1}H NMR analysis revealed the clean and quantitative conversion of the starting dimer into monometallic [RuCl(*p*-cymene)(S_2C·NHC)]Cl complexes. These encouraging results prompted us to perform the reactions on a larger preparative scale. Thus, the ruthenium dimer (0.1 mmol) and 2 equiv of the ligands (0.2 mmol) were weighed in a 10 mL glass vial containing a magnetic stirring bar. A minimum amount of dichloromethane (2−3 mL) was added, and the mixture was stirred for 10 min at room temperature. The volatile solvent was easily removed on a rotary evaporator, and the solid residue was broken down into a fine powder by stirring it in the presence of petroleum ether. The slurry was centrifuged, the supernatant liquid was removed, and the remaining solid was dried under high vacuum. Gratifyingly, almost quantitative yields (97−100%) of pure products were obtained (Scheme 2). The ^{1}H and ^{13}C NMR spectra of compounds **2a−e** were compared with those recorded previously for the analogous [RuCl(*p*-cymene)(S_2C·NHC)]PF_6 salts (**1a−e**).[5] They were quite similar, except for the resonances of the imidazol(in)ium protons, which were strongly influenced by the nature of the counterion (*vide infra*). High-resolution mass spectrometry (ESI, + ve mode) confirmed the correct formulation of the cationic part of these complexes.

Synthesis of Bimetallic [RuCl(*p*-cymene)(S_2C·NHC)]-[$RuCl_3$(*p*-cymene)] Complexes. During our exploratory runs, we recorded the ^{1}H NMR spectrum of a 1:1 mixture of $[RuCl_2(p\text{-cymene})]_2$ and IMes·CS_2 in $CDCl_3$. It revealed the existence of three distinct ruthenium−arene species in solution. Indeed, triplicate resonances with noninteger integrals were detected for all the aromatic and aliphatic protons of the *p*-cymene ligand. This unusual pattern was most visible for the methine protons of the isopropyl groups, which led to three well-separated septets in the ratios 1:0.44:0.56 (Figure 1). The most shielded resonance centered at 2.51 ppm was easily assigned to the [RuCl(*p*-cymene)(S_2C·IMes)]$^+$

https://doi.org/10.1021/acs.inorgchem.1c02648
Inorg. Chem. 2021, 60, 16769−16781

Scheme 2. Synthesis of Monometallic Ruthenium−Arene Complexes 2a−e

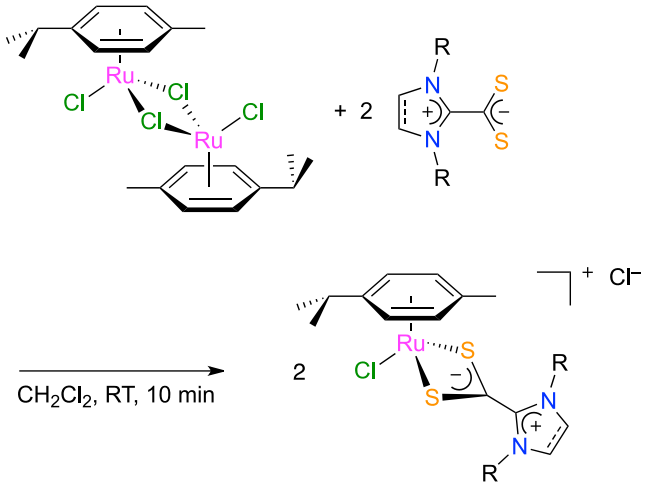

2a: NHC = IMes (100%)
2b: NHC = IDip (98%)
2c: NHC = ICy (97%)
2d: NHC = SIMes (99%)
2e: NHC = SIDip (99%)

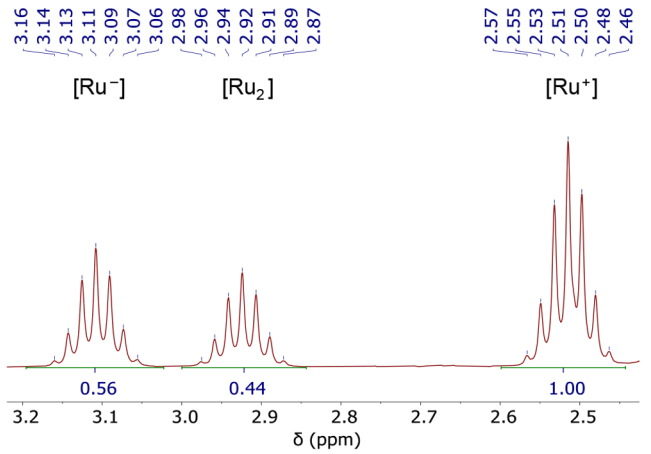

Figure 1. ^{1}H NMR spectrum of a 1:1 stoichiometric mixture of $[RuCl_2(p\text{-cymene})]_2$ and IMes·CS_2 in $CDCl_3$ at 298 K showing the methine protons of the *p*-cymene ligand.

cation by comparison with the spectra recorded for complex **2a** and its hexafluorophosphate analogue **1a**,[5] while the septet located around 2.92 ppm is characteristic of the $[RuCl_2(p\text{-cymene})]_2$ dimer dissolved in $CDCl_3$.[20] The third, unexpected signal observed at 3.11 ppm was attributed to the $[RuCl_3(p\text{-cymene})]^-$ anion to balance the reaction of 1 equiv of dimer with 1 equiv of ligand (eq 1). The nonstoichiometric proportions of the three ruthenium−arene species indicated, however, that the trichlorido(*p*-cymene)ruthenate anion was not formed quantitatively and was therefore in equilibrium with a formal 16-electron species that quickly dimerized into the saturated di-μ-chlorido bridged dimer (eqs 2 and 3). These puzzling observations spurred us to investigate in more detail the course of the reaction between the $[RuCl_2(p\text{-cymene})]_2$ dimer and NHC·CS_2 zwitterions.

$$[RuCl_2(p\text{-cymene})]_2 + NHC{\cdot}CS_2 \rightarrow [RuCl(p\text{-cymene})(S_2C{\cdot}NHC)]^+ + [RuCl_3(p\text{-cymene})]^- \quad (1)$$

$$[RuCl_3(p\text{-cymene})]^- \leftrightarrows [RuCl_2(p\text{-cymene})] + Cl^- \quad (2)$$

$$2[RuCl_2(p\text{-cymene})] \rightarrow [RuCl_2(p\text{-cymene})]_2 \quad (3)$$

$$K_d = \frac{[Ru][Cl^-]}{[Ru^-]} = \frac{(2[Ru_2])([Ru^+] - [Ru^-])}{[Ru^-]} \quad (4)$$

In order to understand how the Ru:NHC·CS_2 ratio influenced the outcome of the complexation, we loaded an NMR tube with the $[RuCl_2(p\text{-cymene})]_2$ homobimetallic dimer (16.1 mg) dissolved in $CDCl_3$ (0.5 mL). Two molar equiv of the IMes·CS_2 ligand (20 mg) were divided into 20 portions of *ca.* 1 mg and added stepwise to this solution. A reaction took place instantaneously at room temperature, and the color of the mixture changed progressively from orange-red to dark and darker shades of red-purple. ^{1}H NMR spectra were recorded after each addition of the ligand (Figure 2). The

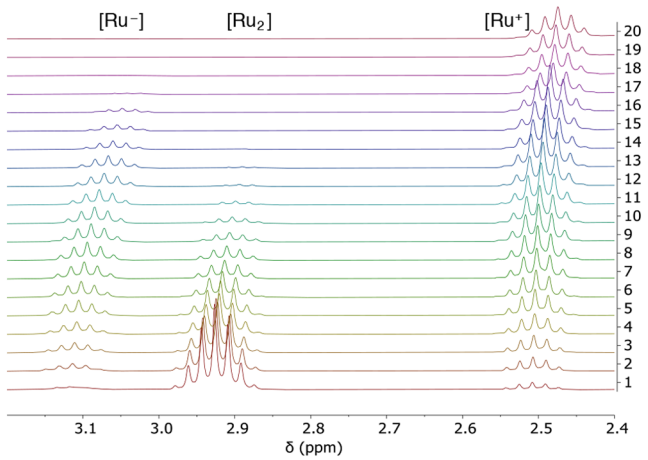

Figure 2. Stacked ^{1}H NMR spectra obtained upon stepwise addition of IMes·CS_2 (2 equiv) to $[RuCl_2(p\text{-cymene})]_2$ in $CDCl_3$ at 298 K showing the methine protons of the *p*-cymene ligand.

three septets arising from the *p*-cymene methine protons located between 2.4 and 3.2 ppm were integrated using the peak of residual $CHCl_3$ at 7.26 ppm as an internal standard. The data obtained were plotted on a graph where the *x* axis represented the percentage of IMes·CS_2 added to the reaction mixture (100% corresponds to 2 equiv of ligand per ruthenium dimer), and the *y* axis corresponded to the percentage of each ruthenium−arene complex with respect to the sum of all three cationic, neutral, and anionic species (Figure 3).

The linear correlation observed in Figure 3 for the formation of the $[RuCl(p\text{-cymene})(S_2C{\cdot}IMes)]^+$ cation with respect to the amount of zwitterion added to the reaction medium nicely confirmed that the chelation of the dithiocarboxylate ligand occurred quickly and irreversibly with no induction period, as described in eq 1. Conversely, the nonlinear consumption of the $[RuCl_2(p\text{-cymene})]_2$ dimer and the transient formation of the $[RuCl_3(p\text{-cymene})]^-$ anion corroborated the existence of an equilibrium between these two species, as described in eqs 2 and 3. Such a dissociation equilibrium was already evidenced by Vock and Dyson when they prepared the $Ph_4P[RuCl_3(p\text{-cymene})]$ complex[21] and by Robertson and Stephenson when they synthesized the related $Cs[RuCl_3(benzene)]$ salt.[22] We have determined the dissociation constant (K_d) of the $[RuCl_3(p\text{-cymene})]^-$ anion from the relative concentrations of the three ruthenium−arene species obtained by integrating

https://doi.org/10.1021/acs.inorgchem.1c02648
Inorg. Chem. 2021, 60, 16769−16781

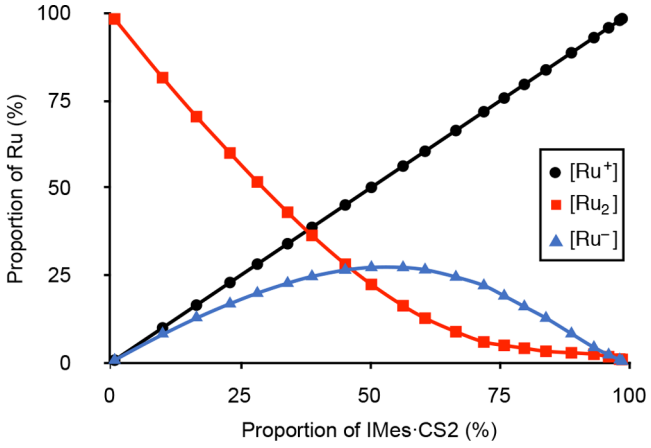

Figure 3. Evolution of the relative proportions of cationic [RuCl(*p*-cymene)(S_2C·IMes)]$^+$ ("[Ru^+]"), neutral [Ru_2Cl_2(*p*-cymene)]$_2$ ("[Ru_2]"), and anionic [$RuCl_3$(*p*-cymene)]$^-$ ("[Ru^-]") complexes as a function of the Ru:IMes·CS_2 ratio (100% corresponds to 2 equiv of ligand per ruthenium dimer).

their methine protons for various Ru:IMes·CS_2 ratios (eq 4, see the Supporting Information for computational details). At 25 °C in $CDCl_3$, K_d = 0.02 mol L^{-1}. Lowering the temperature to 0 °C or increasing it to 50 °C did not significantly alter this value. Contrastingly, replacing $CDCl_3$ with either a less polar solvent (CD_2Cl_2) or a more polar, protic solvent (CD_3OD) significantly altered the equilibrium between the neutral and the anionic species (Figure 4). Hence, the almost statistical

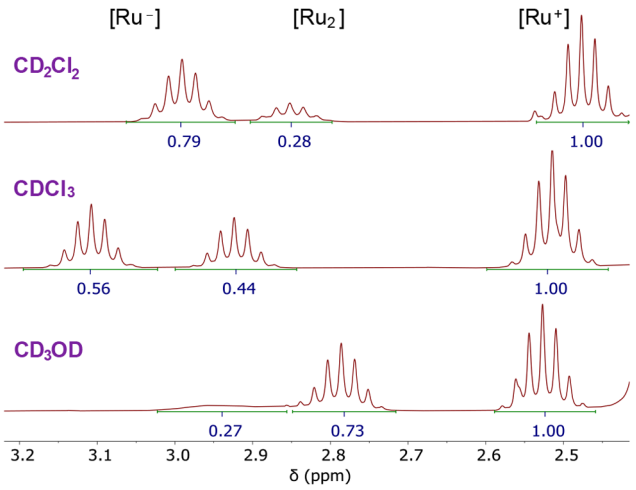

Figure 4. ^{1}H NMR spectra of a 1:1 stoichiometric mixture of [$RuCl_2$(*p*-cymene)]$_2$ and IMes·CS_2 in CD_2Cl_2 (top), $CDCl_3$ (middle), and CD_3OD (bottom) at 298 K showing the methine protons of the *p*-cymene ligand.

distribution between the [$RuCl_3$(*p*-cymene)]$^-$ and the Cl^- anions observed in chloroform at room temperature (a 56:44 ratio) was shifted toward the former ruthenate complex in dichloromethane (74:26) or toward the later inorganic anion in methanol (27:73). In DMSO-d_6, only the cationic complex **2a** and the neutral [$RuCl_2$(*p*-cymene)(DMSO-d_6)] solvate were detected, which corresponded to a (0:100) distribution in favor of the chloride counteranion (Figure 5). Spectra recorded in D_2O were more difficult to interpret. This is most likely due to the occurrence of aquation reactions

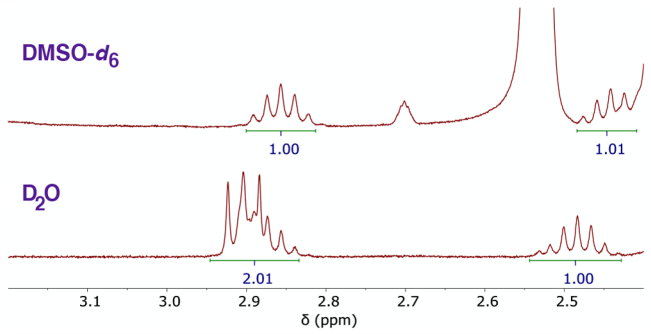

Figure 5. ^{1}H NMR spectra of a 1:1 stoichiometric mixture of [$RuCl_2$(*p*-cymene)]$_2$ and IMes·CS_2 in DMSO-d_6 (top) and D_2O (bottom) at 298 K showing the methine protons of the *p*-cymene ligand.

involving the labile Ru−Cl bonds of the anionic, neutral, or cationic ruthenium−arene species. Indeed, the behavior of the [$RuCl_2$(arene)]$_2$ dimers in the presence of water has been cross-examined since the 1970s.[23] Eventually, the [$RuCl_2(C_6H_6)$]$_2$ complex was shown to afford three aquation products in D_2O, *viz.*, [$RuCl_2(C_6H_6)(D_2O)$], [$RuCl(C_6H_6)(D_2O)_2$]$^+$, and [$Ru(C_6H_6)(D_2O)_3$]$^{2+}$.[24] The reactivity of numerous monometallic [$RuCl_2$(arene)L] complexes toward DMSO[25] and water[26] has also been extensively investigated, because it critically affects the biological activity of these metallodrugs.

In order to isolate and to characterize the bimetallic [RuCl(*p*-cymene)(S_2C·NHC)][$RuCl_3$(*p*-cymene)] complexes, we performed reactions on a preparative scale starting from an equimolar mixture of the [$RuCl_2$(*p*-cymene)]$_2$ dimer and an NHC·CS_2 zwitterion (0.1 mmol each). The two reagents were weighed in a 10 mL glass vial containing a magnetic stirring bar, and dichloromethane (3 mL) was added. The mixture was stirred for 10 min at room temperature. The solvent was removed on a rotary evaporator, and the solid residue was broken down into a fine powder by stirring it in the presence of petroleum ether. The slurry was decanted, the supernatant liquid was removed, and the remaining solid was dried under high vacuum. This straightforward procedure that did not involve any filtration or transfer into another container allowed us to prepare a set of five dual anionic and cationic complexes (**3a−e**) in almost quantitative yields (95−100%) (Scheme 3).

Cabeza and co-workers first disclosed the synthesis and the molecular structure of the trichlorido(*p*-cymene)ruthenate anion associated with a dipyridinium cation in 2005.[27] The year after, Vock and Dyson prepared the phosphonium salt Ph_4P[$RuCl_3$(*p*-cymene)] and solved its solid-state structure.[21] Subsequently, several other research groups carried out the synthesis of mixed organic/organometallic salts combining the [$RuCl_3$(*p*-cymene)]$^-$ anion with tetrahydropyrimidinium,[28] imidazolium,[29] ammonium,[30] phenothiazinium,[31] or guanidinium cations.[32] To the best of our knowledge, prior to this work, only five reports from the literature described salts in which both the anion and the cation were ruthenium−(*p*-cymene) complexes (Chart 2). In many cases, they were obtained adventitiously instead of the targeted monometallic products. Thus, in 2006, Dyson et al. fortuitously crystallized the [RuCl(*p*-cymene)(bimid)$_2$][$RuCl_3$(*p*-cymene)] complex **4** (bimid is *N*-butylimidazole) in a failed attempt to obtain the neutral [$RuCl_2$(*p*-cymene)(bimid)] derivative.[33] Then, in 2008, Marchetti, Pettinari, and co-workers prepared a set of

https://doi.org/10.1021/acs.inorgchem.1c02648
Inorg. Chem. 2021, 60, 16769−16781

Scheme 3. Synthesis of Dual Anionic and Cationic Ruthenium−Arene Complexes 3a−e

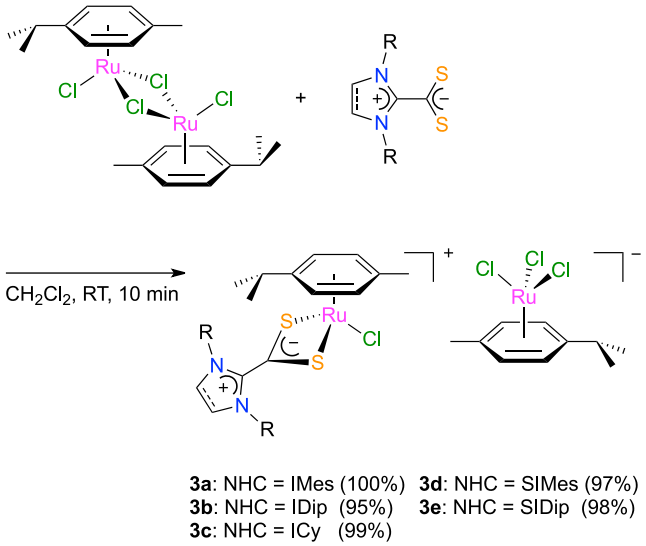

three [RuCl(*p*-cymene)(N^N)][$RuCl_3$(*p*-cymene)] complexes **5a−c** with various bis(pyrazolyl)alkane (N^N) ligands.[34] One example of [RuCl(*p*-cymene)(semicarbazone)][$RuCl_3$(*p*-cymene)] salt (**6**)[35] and three related thiosemicarbazone derivatives (**7a−c**)[36] originated from the groups of Su and Li, while an additional compound, [RuCl(*p*-cymene)(1-FcMeIm)$_2$][$RuCl_3$(*p*-cymene)] (**8**), was unexpectedly formed when Walsby et al. tried to crystallize the [$RuCl_2$(*p*-cymene)(1-FcMeIm)] complex (1-FcMeIm is 1-ferrocenyl-(methyl)imidazole).[37] Apart from *p*-cymene, benzene was the only other arene succinctly investigated for the preparation of ruthenate complexes, with an early report from Robertson and Stephenson describing the synthesis of Cs[$RuCl_3$(benzene)][22] and only two examples of dual anionic and cationic ruthenium−benzene complexes, *viz.*, a bis(pyrazolyl) derivative analogous to products **5a−c** described by Marchetti, Pettinari, and co-workers in 2008,[34] and the chiral compound **9** serendipitously crystallized by Tamm et al. in 2014.[38]

Structural Analysis. Various analytical techniques were applied to fully characterize complexes **3a−e**. As discussed above (*cf.* Figure 1), they displayed three sets of signals for the various aliphatic and aromatic protons of *p*-cymene on ^{1}H NMR spectroscopy. These resonances were assigned, respectively, to the [RuCl(*p*-cymene)(S_2C·NHC)]$^+$ cations and to a mixture of [$RuCl_3$(*p*-cymene)]$^-$ anions in equilibrium with the [$RuCl_2$(*p*-cymene)]$_2$ dimer. ^{1}H and ^{13}C NMR analyses also confirmed the successful incorporation of an imidazol(in)ium-2-dithiocarboxylate ligand in the bimetallic compounds under scrutiny. In particular, the strongly deshielded resonance of the CS_2^- unit observed at 213−220 ppm clearly evidenced the chelation of an NHC·CS_2 zwitterion to a ruthenium center (Table 1). Indeed, this diagnostic signal

Table 1. ^{13}C NMR Chemical Shifts (ppm) of the CS_2^- Unit of NH·CS_2 Zwitterions in Various Cationic Complexes of the [RuCl(*p*-cymene)(S_2C·NHC)]$^+$ Type and in the Free Ligands[a]

NHC	NHC·CS_2[b]	[Ru$^+$](PF_6^-) (**1**)[c]	[Ru$^+$](Cl^-) (**2**)	[Ru$^+$][Ru^-] (**3**)
IMes (**a**)	221.6[d]	212.4	212.2	214.2
IDip (**b**)	219.7	211.8	211.8	213.2
ICy (**c**)	226.0	218.1	218.8	220.2
SIMes (**d**)	222.7	213.1	213.9	215.8
SIDip (**e**)	219.8	211.8	211.7	213.3

[a]Data recorded in $CDCl_3$ at 298 K. [b]Data from ref 2. [c]Data from ref 5. [d]Data recorded in DMSO-d_6 at 298 K.

was detected at the same location in monometallic complexes **1a−e** (212−218 ppm)[5] and **2a−e** (212−219 ppm). Besides, there was always a small albeit significant upfield shift (*ca.* 6 ppm) between these values and those recorded for the free, uncoordinated betaines (220−226 ppm).[2] Most of the other ^{1}H and ^{13}C resonances arising from the [RuCl(*p*-cymene)-(S_2C·NHC)]$^+$ moiety were also rather similar, whether we looked at the NMR spectra of compounds **1a−e**, **2a−e**, or **3a−e**. A change in the counterion nature, however, markedly influenced the chemical shifts of the imidazol(in)ium ring protons in the three types of cationic complexes under investigation (Table 2). Thus, the chemical shifts of the aromatic protons on the imidazolium rings of IMes·CS_2, IDip·CS_2, or ICy·CS_2 drifted from *ca.* 7 ppm in the free ligands to more than 8 ppm in mono- and bimetallic complexes **2a−c** and

Chart 2. Dual Anionic and Cationic Ruthenium−Arene Complexes Known Prior to This Work

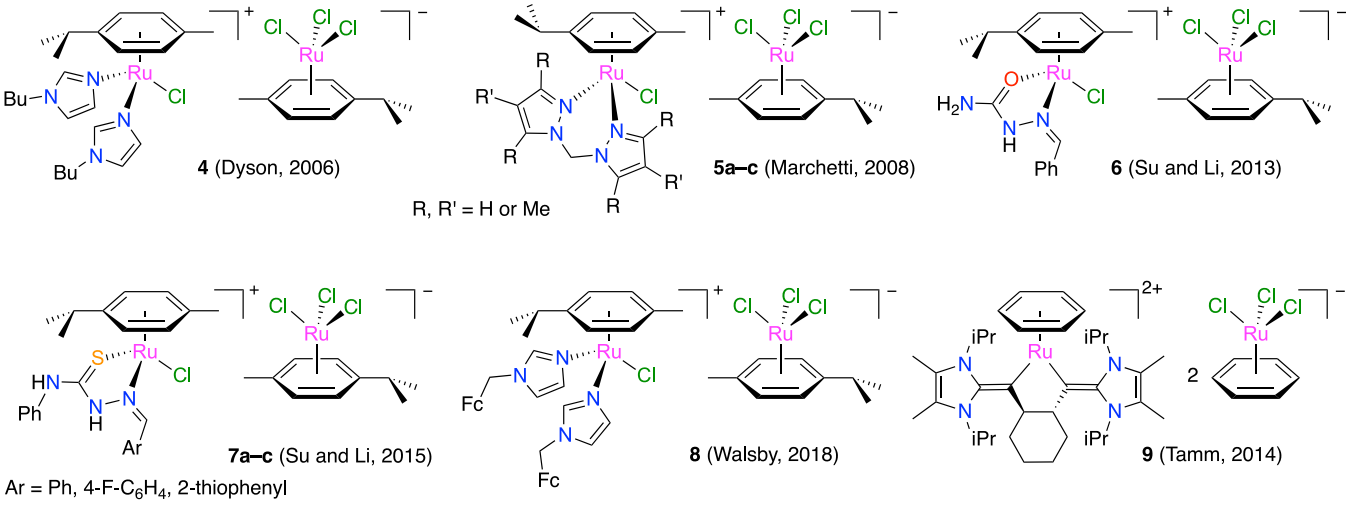

https://doi.org/10.1021/acs.inorgchem.1c02648
Inorg. Chem. 2021, 60, 16769−16781

Table 2. ^{1}H NMR Chemical Shifts (ppm) of the Imidazol(in)ium Protons in the Free Ligands and in Various Cationic Complexes of the [RuCl(*p*-cymene)(S_2C·NHC)]$^+$ Type[a]

NHC	NHC·CS_2[b]	[Ru^+](PF_6^-) (**1**)[c]	[Ru^+](Cl^-) (**2**)	[Ru^+][Ru^-] (**3**)
IMes (**a**)	7.84[d]	7.57	8.25	8.30
IDip (**b**)	7.01	7.71	8.39	8.49
ICy (**c**)	6.99	7.53	8.13	8.06
SIMes (**d**)	4.20	4.32	4.64	4.64
SIDip (**e**)	4.41	4.42	4.68	4.65

[a]Data recorded in $CDCl_3$ at 298 K. [b]Data from ref 2. [c]Data from ref 5. [d]Data recorded in DMSO-d_6 at 298 K.

3a−c, with intermediate values in compounds **1a−c**. The nonaromatic backbone of the imidazolinium-based ligands SIMes·CS_2 and SIDip·CS_2 underwent a less dramatic downfield move, with chemical shifts varying from 4.20 and 4.41 ppm in the free ligands to 4.64 and 4.65 ppm in complexes **3d,e**. These variations reveal the existence of strong interactions between the azolium ring and the counteranion of compounds **1−3** in solution. As expected, the trichlorido(*p*-cymene)ruthenate complex or a single chloride anion were more influential than a weakly coordinating hexafluorophosphate anion.[39]

The FT-IR spectra of bimetallic complexes **3a−e** were recorded in KBr pellets and compared with those reported previously for monometallic complexes **1a−e**[5] and for the parent uncoordinated NHC·CS_2 zwitterions[2] (Table 3). Similar patterns were observed for the three types of compounds. In addition to the various aliphatic and aromatic C−H stretching vibration bands located around 3000 cm^{-1}, the most intense absorption originating from the [RuCl(*p*-cymene)(S_2C·NHC)]$^+$ cations came from the asymmetric stretching of the N_2C^+ groups, which gave rise to a strong band located at *ca.* 1475 cm^{-1} for the aromatic imidazolium derivatives and at *ca.* 1545 cm^{-1} for their imidazolinium counterparts. Due to the poor electronic communication between the azolium ring and the orthogonal dithiocarboxylate unit of bulky NHC·CS_2 zwitterions, these bands were not significantly affected by the complexation process. Conversely, a substantial shift of the CS_2^- asymmetric stretching vibration bands to lower energies occurred upon chelation of the dithiocarboxylate inner salts to ruthenium, together with a notable decrease in their intensity. This attenuation did not allow us to identify them with certainty in all cases. Hence, the $\bar{\nu}_{asym}$ (CS_2^-) values listed in Table 3 should be treated with circumspection and not overly interpreted.

Positive HR-ESI-MS spectra of complexes **3a−e** recorded in acetonitrile were very clean and similar to those recorded for the monometallic complexes **2a−e**. They featured only a single signal unambiguously assigned to an [RuCl(*p*-cymene)(S_2C·NHC)]$^+$ molecular ion based on its isotopic profile (see the Supporting Information for details). In the negative mode, a peak at m/z = 340.92101 corresponding to the [$RuCl_3$(*p*-cymene)]$^-$ anion was always detected, but its intensity was rather low; and other unidentified species were sometimes observed. These results are in line with a facile dissociation of the labile ruthenate complex and the formation of other ruthenium species in the ionization chamber. We did not characterize complexes **3a−e** by elemental analysis, because of their strong tendency to cocrystallize with various solvents in an unpredictable manner.

X-ray Crystallography. Attempts to crystallize complexes **3a−e** by slow diffusion of petroleum ether in a dichloromethane solution at 6 °C under the exclusion of air and moisture were not successful. However, water turned out to be a good solvent for these compounds (*vide infra*), and we ventured to crystallize them from water/organic solvent mixtures. Gratifyingly, a crystalline sample of [RuCl(*p*-cymene)(S_2C·IMes)][$RuCl_3$(*p*-cymene)] (**3a**) was obtained from acetone/water. X-ray diffraction analysis revealed that the anionic and cationic ruthenium−arene fragments had cocrystallized with one molecule of H_2O (Figure 6). We were also able to grow monocrystals of the analogous SIMes-based complex **3d** from a dichloromethane solution saturated with water. In this case, the bimetallic complex cocrystallized with H_2O in a 2:3 stoichiometric ratio (Figure 7).

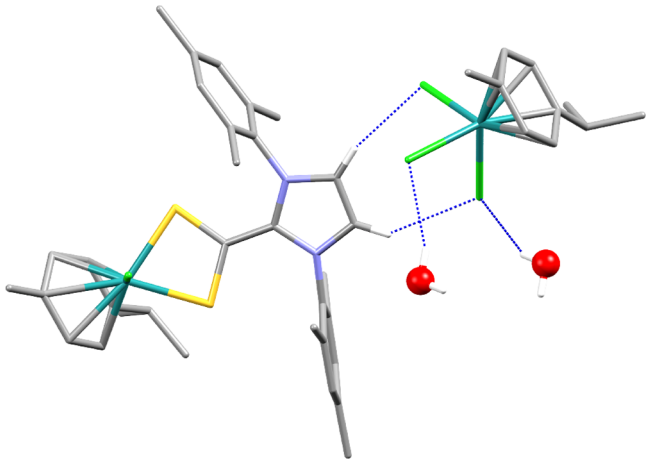

Figure 6. Molecular structure of [RuCl(*p*-cymene)(S_2C·IMes)]-[$RuCl_3$(*p*-cymene)] cocrystallized with water (**3a**·H_2O) showing the H-bonds of the imidazolium protons (hydrogen atoms were omitted except those directly bound to the heterocyclic ring and oxygen).

Table 3. Wavenumbers of IR Stretching Vibration Bands (cm^{-1}) in the Free Ligands and in Various Cationic Complexes of the [RuCl(*p*-cymene)(S_2C·NHC)]$^+$ Type[a]

NHC	$\bar{\nu}_{asym}$ (N_2C^+) in NHC·CS_2[b]	$\bar{\nu}_{asym}$ (N_2C^+) in [Ru^+](PF_6^-) (**1**)[c]	$\bar{\nu}_{asym}$ (N_2C^+) in [Ru^+][Ru^-] (**3**)	$\bar{\nu}_{asym}$ (CS_2^-) in NHC·CS_2[b]	$\bar{\nu}_{asym}$ (CS_2^-) in [Ru^+](PF_6^-) (**1**)[c]	$\bar{\nu}_{asym}$ (CS_2^-) in [Ru^+][Ru^-] (**3**)
IMes (**a**)	1488	1485	1484	1052	1025	1009
IDip (**b**)	1469	1470	1468	1058	1010	1001
ICy (**c**)	1474	1474	1469	1058	1029	1026
SIMes (**d**)	1531	1559	1553	1064	1032	1031
SIDip (**e**)	1524	1549	1541	1080	1058	1055

[a]Data recorded in KBR pellets. [b]Data from ref 2. [c]Data from ref 5.

https://doi.org/10.1021/acs.inorgchem.1c02648
Inorg. Chem. 2021, 60, 16769−16781

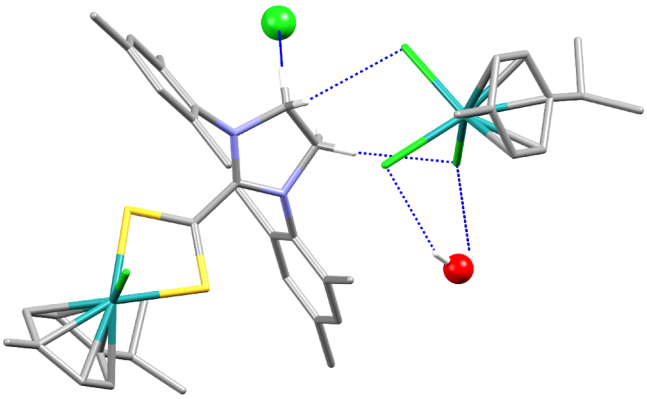

Figure 7. Molecular structure of [RuCl(*p*-cymene)(S_2C·SIMes)]-[$RuCl_3$(*p*-cymene)] cocrystallized with water (2(**3d**)·3(H_2O)) showing the H-bonds of the imidazolinium protons (hydrogen atoms were omitted except those directly bound to the heterocyclic ring and oxygen).

A close examination of the solid materials obtained from the crystallization of **3a** in acetone/water showed that they contained a small amount of green crystals that turned out to be the hydrated complex **2a**, as evidenced by XRD analysis (Figure 8). Moreover, the slow evaporation of a dichloro-

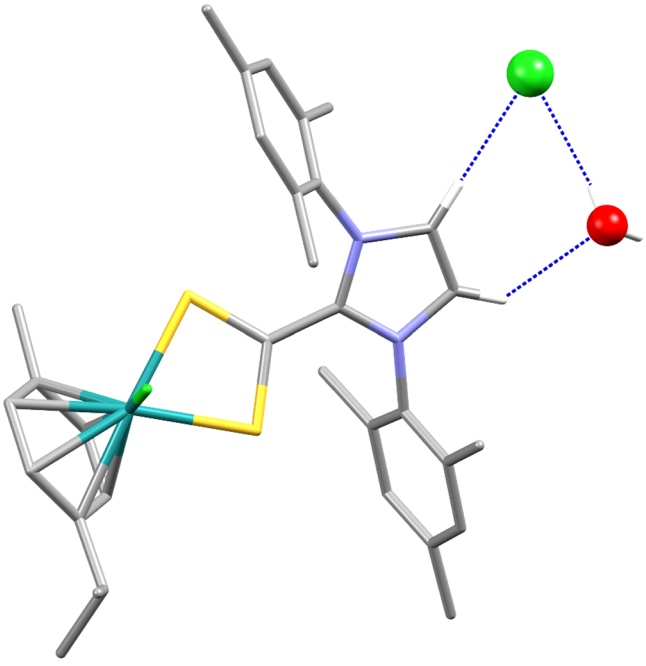

Figure 8. Molecular structure of [RuCl(*p*-cymene)(S_2C·IMes)]Cl cocrystallized with water (**2a**·H_2O) showing the H-bonds of the imidazolium protons (hydrogen atoms were omitted except those directly bound to the heterocyclic ring and oxygen).

methane solution of [RuCl(*p*-cymene)(S_2C·ICy)][$RuCl_3$(*p*-cymene)] (**3c**) in the presence of moisture led to the isolation of orange crystals whose molecular structure determined by XRD analysis corresponded to a hydrated chloride salt with the formula 2(**2c**)·9.75(H_2O) (Figure 9). A powder diffractogram of the bulk solid mass out of which these crystals where handpicked revealed the presence of another compound not suitable for single-crystal analysis that was probably the bimetallic complex **3c** (see the Supporting Information for

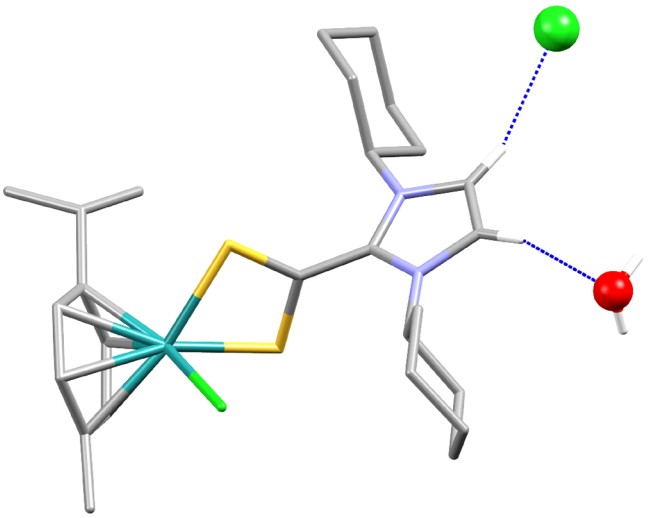

Figure 9. Molecular structure of [RuCl(*p*-cymene)(S_2C·ICy)]Cl cocrystallized with water (2(**2c**)·9.75(H_2O)) showing the H-bonds of the imidazolium protons (hydrogen atoms were omitted except those directly bound to the heterocyclic ring and oxygen).

details). Last but not least, only the [$RuCl_2$(*p*-cymene)]$_2$ dimer was detected by XRD analysis in a sample of complex **3b** subjected to crystallization. All these results are in line with a reversible dissociation of the [$RuCl_3$(*p*-cymene)]$^-$ anion into Cl^- and [$RuCl_2$(*p*-cymene)]$_2$ during the crystallization process. When crystals of pure bimetallic complexes **3a**·H_2O and 2(**3d**)·3(H_2O) containing the trichlorido(*p*-cymene)-ruthenate counteranion were dissolved in CD_2Cl_2 or $CDCl_3$, NMR analyses confirmed that an equilibration had taken place, and the three cationic, neutral, and anionic ruthenium−arene species were present in solution (*cf.* Figure 1).

The cationic parts of complexes **2a**, **3a**, **2c**, and **3d** displayed the typical three-legged piano stool geometry already evidenced in complex **1a** and in many other ruthenium−arene species.[40] In these four compounds, the S1−C1−S2 bite angle of the dithiocarboxylate unit averaged 112° (Table 4 and Figure 10). The C1−S1 and C1−S2 distances were very similar, and their lengths (1.68 Å) were much closer to the distance commonly observed for C═S double bonds (1.67 Å) than for C−S single bonds (1.75 Å),[41] in line with the uniform delocalization of a negative charge between the two sulfur atoms. Likewise, the N1 and N2 nitrogen atoms were almost equally spaced from the central C2 carbon atom, thereby indicating similar contributions of the N1−C2═$N2^+$ and $^+$N1═C2−N2 resonance forms to the amidinium functionality. As expected, the replacement of IMes·CS_2 or ICy·CS_2 with the imidazolinium-2-dithiocarboxylate zwitterion SIMes·CS_2 in complex **3d** significantly impacted the C3−C4 distance and the N1−C2−N2 angle, due to the saturation of its heterocyclic backbone. Other geometric parameters remained roughly unchanged.

The bond lengths and angles recorded for the [RuCl(*p*-cymene)(S_2C·IMes)]$^+$ cation in the molecular structures of **1a**, **2a**·H_2O, and **3a**·H_2O were not significantly altered by a change in the nature of the counterion or the cocrystallized solvent. Yet, variations in the relative orientations of the carbene and arene ligands and of the dithiocarboxylate and mesityl groups with respect to the central imidazolium ring of the NHC ligand were evidenced when comparing the relevant torsion angles (Table 4 and Figure 10). These discrepancies are a likely

https://doi.org/10.1021/acs.inorgchem.1c02648
Inorg. Chem. 2021, 60, 16769−16781

Table 4. Selected Bond Lengths (Å) and Angles (deg) for the [RuCl(*p*-cymene)(S_2C·NHC)]$^+$ Cations Derived from the Crystal Structures of [RuCl(*p*-cymene)(S_2C·IMes)]PF_6 (1a), [RuCl(*p*-cymene)(S_2C·IMes)]Cl (2a), [RuCl(*p*-cymene)(S_2C·IMes)][$RuCl_3$(*p*-cymene)] (3a), RuCl(*p*-cymene)(S_2C·ICy)]Cl (2c), and [RuCl(*p*-cymene)(S_2C·SIMes)][$RuCl_3$(*p*-cymene)] (3d)[a]

complex	C1−S1	C1−S2	C1−C2	C2−N1	C2−N2	C3−C4	Ru1−Cl1	Ru1−cym	Cl1−Ru1−C23−C29
1a[b]	1.680(3)	1.673(2)	1.464(3)	1.351(3)	1.342(3)	1.324(4)	2.4128(9)	1.710	−6.3(2)
2a·H_2O	1.679(2)	1.681(2)	1.455(3)	1.358(3)	1.351(3)	1.348(3)	2.3977(5)	1.689(9)	79.0(2)
3a·H_2O	1.688(5)	1.683(6)	1.435(8)	1.355(7)	1.349(7)	1.352(8)	2.3887(16)	1.705(3)	−11.7(5)
2(**2c**)·9.75(H_2O)	1.675(3)	1.681(3)	1.474(5)	1.344(4)	1.333(5)	1.345(5)	2.4140(9)	1.697(2)	−23.0(3)
2(**3d**)·3(H_2O)	1.674(6)	1.678(6)	1.481(9)	1.321(8)	1.311(8)	1.519(8)	2.390(2)	1.705(3)	−13.0(5)

complex	S1−C1−S2	N1−C2−N2	S1−C1−C2−N1	C2−N1−C5−C6	C2−N2−C14−C15	S1−Ru1−S2	S1−Ru1−Cl1
1a[b]	112.3(1)	107.3(2)	45.0(4)	−102.6(3)	77.8(3)	71.69(2)	86.24(2)
2a·H_2O	112.3(1)	106.9(2)	30.5(3)	73.7(3)	−117.8(2)	71.79(2)	87.75(2)
3a·H_2O	110.3(3)	106.3(5)	16.2(8)	77.9(7)	−90.1(7)	72.07(5)	84.08(6)
2(**2c**)·9.75(H_2O)	111.9(2)	108.2(3)	−87.4(4)			71.90(3)	85.98(3)
2(**3d**)·3H_2O	112.4(4)	113.8(6)	36.9(8)	74.0(8)	−111.4(7)	72.10(6)	84.73(6)

[a]See Figure 10 for atom labeling. [b]Data from ref 5.

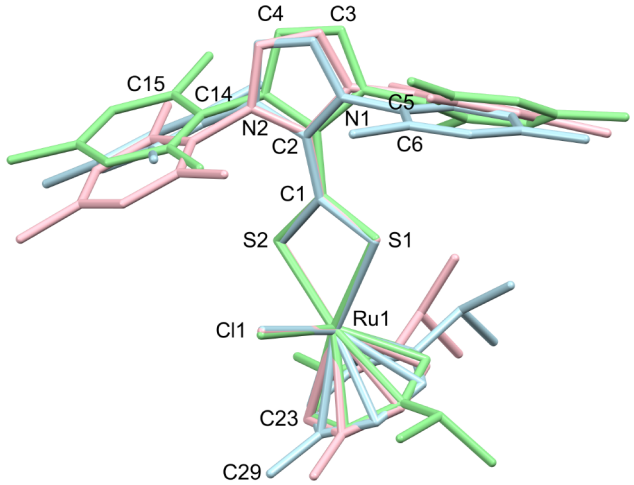

Figure 10. Conformations of the [RuCl(*p*-cymene)(S_2C·IMes)]$^+$ cation in the molecular structures of complexes **1a** (pink), **2a**·H_2O (green), and **3a**·H_2O (blue).

consequence of the conformational changes needed to accommodate neighboring counteranions of different sizes and solvent molecules in the crystal structure. The rotational freedom of the arene ligand was particularly striking. Indeed, the bulky isopropyl substituent of *p*-cymene was approximately *anti* to the chlorido ligand in complexes **1a**, **3a**, **2c**, and **3d**, whereas it adopted a gauche conformation in the solid-state structure of **2a**.

Metrics determined for the [$RuCl_3$(*p*-cymene)]$^-$ anion from the molecular structures of complexes **3a** and **3d** were in good agreement with those reported previously for mixed organic/organometallic salts[21,27−32] and dual anionic and cationic complexes[33,35−37] featuring this moiety. The ruthenium atom exhibited a distorted octahedral geometry with the aromatic ring of the *p*-cymene ligand formally occupying three coordination sites and the three chlorido ligands occupying the remaining three facial positions. Hence, a typical piano stool geometry was again evidenced for this assembly. The Ru−Cl bond lengths averaged 2.43 Å, and the Cl−Ru−Cl angles were close to 90° (Table 5). At 1.64 Å, the distance between the metal center and the centroid of the arene ring was slightly shorter than in the cationic moiety, where it reached 1.70 Å (*cf.* Table 4). The deviation of planarity between the methyl group of *p*-cymene and the nearest chlorido ligand equaled 20° in the [$RuCl_3$(*p*-cymene)]$^-$ anion, irrespective of the accompanying cation and number of cocrystallized water molecules, thereby leading to a staggered conformation (Figure 11).

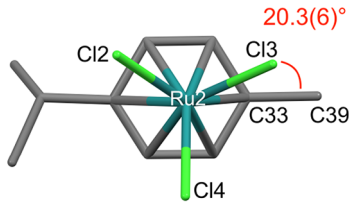

Figure 11. View of the [$RuCl_3$(*p*-cymene)]$^-$ anion in the molecular structure of complex **3d** showing its staggered conformation.

An examination of the close contacts between the cation, the anion, and the solvent in the various molecular structures under scrutiny revealed the existence of strong interactions between the azolium ring protons and neighboring *n*- or *π*-donors (Table 6). At least one of the hydrogens of the positively charged heterocycle was always directly bonded to an heteroatom from the counteranion, whether it was a fluorine atom from PF_6^- in **1a**, the Cl^- anion in **2a** and **2c** (Figures 8 and 9), or a chlorido ligand from [$RuCl_3$(*p*-

Table 5. Selected Bond Lengths (Å) and Angles (deg) for the [$RuCl_3$(*p*-cymene)]$^-$ Anion Derived from the Crystal Structures of RuCl(*p*-cymene)(S_2C·IMes)][$RuCl_3$(*p*-cymene)] (3a) and [RuCl(*p*-cymene)(S_2C·SIMes)][$RuCl_3$(*p*-cymene)] (3d)[a]

complex	Ru2−Cl2	Ru2−Cl3	Ru2−Cl4	Ru2−cym	Cl2−Ru2−Cl3	Cl2−Ru2−Cl4	Cl3−Ru2−C33−C39
3a·H_2O	2.4337(16)	2.4300(14)	2.4176(16)	1.641(3)	89.27(5)	88.10(6)	−20.2(5)
2(**3d**)·3H_2O	2.4186(17)	2.4397(17)	2.4416(18)	1.648(3)	88.00(6)	87.40(6)	20.3(6)

[a]See Figure 11 for atom labeling.

https://doi.org/10.1021/acs.inorgchem.1c02648
Inorg. Chem. 2021, 60, 16769−16781

Table 6. Selected Bond Lengths (Å) and Angles (deg) for the Hydrogen Bonds between the Azolium Ring Protons and the Counteranions or Solvent Molecules Derived from the Crystal Structures of [RuCl(*p*-cymene)(S_2C·IMes)]PF_6 (**1a**), [RuCl(*p*-cymene)(S_2C·IMes)]Cl (**2a**), [RuCl(*p*-cymene)(S_2C·IMes)][$RuCl_3$(*p*-cymene)] (**3a**), [RuCl(*p*-cymene)(S_2C·ICy)]Cl (**2c**), and [RuCl(*p*-cymene)(S_2C·SIMes)][$RuCl_3$(*p*-cymene)] (**3d**)

complex	Donor−H···Acceptor	D−H	H···A	D···A	D−H···A
1a[a]	C4−H4···F45	0.93	2.54	3.356(4)	147
	C3−H3···Mes	0.93	2.98	3.878	162
2a·H_2O	C4−H4···Cl2	0.95	2.57	3.451(2)	154
	C3−H3···O1	0.95	2.58	3.131(3)	117.5
3a·H_2O	C3−H3···Cl4	0.95	2.66	3.453(6)	141.1
	C4−H4···Cl2	0.95	2.55	3.414(6)	151.8
2(**2c**)·9.75(H_2O)	C3−H3···Cl2	0.95	2.56	3.476(4)	161.4
	C4−H4···O2W	0.95	2.49	3.403(6)	162.1
2(**3d**)·3H_2O	C3−H3B···Cl4[b]	0.99	2.60	3.554(7)	162.7
	C4−H4A···Cl2[b]	0.99	2.83	3.398(6)	117.4
	C4−H4B···Cl1[c]	0.99	2.72	3.553(7)	141.5

[a]Data from ref 5. [b]Symmetry code: −1/2 + *x*, *y*, 3/2 − *z*. [c]Symmetry code: 3/2 − *x*, 1/2 + *y*, *z*.

cymene)]$^-$ in **3a** and **3d** (Figures 6 and 7). Additional hydrogen bonding from the imidazolium or imidazolinium protons occurred with water molecules in **2a** and **2c**, with other chlorido ligands from [$RuCl_3$(*p*-cymene)]$^-$ in **3a** and **3d**, and through π-stacking with the mesityl ring of a neighboring cation in **1a**. Although these supramolecular associations were observed in the solid state, they should be preserved to some extent in solution to justify the large differences of chemical shifts evidenced by ^{1}H NMR spectroscopy when monitoring the resonances of the azolium backbone protons (*cf.* Table 2). Advanced NMR and DFT techniques were successfully applied to quantify the ion pairing in other cationic ruthenium−(*p*-cymene) complexes,[42] but we did not further investigate this issue. For the sake of completeness, it should be mentioned that H-bonds were also detected between the cocrystallized water molecules and the counteranions of complexes **2a**, **3a**, **2c**, and **3d** (see the Supporting Information for details).

Water Solubility. During the course of this work, several experimental observations strongly suggested that ruthenium−arene complexes bearing imidazol(in)ium-2-dithiocarboxylate ligands had a strong affinity toward water (*vide supra*). Hence, we decided to investigate more thoroughly this remarkable property by determining the aqueous solubility of monometallic complexes **2a**−**e** and their bimetallic analogues **3a**−**e**. A simple and straightforward procedure was applied for these tests. Distilled water was added in small portions (0.05 mL) to 5 μmol of each complex at room temperature. The mixture was vigorously shaken after every addition, and the process was repeated until no more solid was visible. Very gratifyingly, millimolar concentrations of the various compounds under investigation could be achieved in water (Table 7), and the dark orange-brown solutions obtained were stable for extended periods of time (up to several months) in the presence of oxygen and light. It should be pointed out that the starting azolium-2-dithiocarboxylate inner salts were insoluble in water despite their zwitterionic nature. Except for the SIDip·CS_2 ligand, dual anionic and cationic complexes **3a**−**d** were significantly more soluble than the corresponding monometallic compounds **2a**−**d**. These results demonstrate that the [$RuCl_3$(*p*-cymene)]$^-$ counterion is a valuable alternative to the chloride anion for ensuring a high solubility of cationic ruthenium−arene complexes in water. Among the ten compounds screened, complex **3a** that featured the IMes·CS_2 ligand displayed the highest solubility, leading to a 0.01 M saturated solution in water. This corresponds to a 0.02 M concentration in metal species. Although these values are not exceptional, they compare favorably with solubilities in the 0.1−5 mM range previously reported for various other ruthenium−arene complexes.[43] Besides, they are more than sufficient to enable biological studies in aqueous media and to circumvent hypothetical drug delivery problems.

Table 7. Solubility (mM) of the [RuCl(*p*-cymene)(S_2C·NHC)]Cl Complexes (**2a**−**e**) and the [RuCl(*p*-cymene)(S_2C·NHC)][$RuCl_3$(*p*-cymene)] Complexes (**3a**−**e**) in Distilled Water at Room Temperature

NHC	[Ru^+](Cl^-) (**2**)	[Ru^+][Ru^-] (**3**)
IMes (**a**)	5.6	10
IDip (**b**)	4.6	5.6
ICy (**c**)	3.1	5.0
SIMes (**d**)	2.6	2.8
SIDip (**e**)	5.0	3.3

Biological Activity. Although the cytotoxic effects of ruthenium complexes have been known since the early 1950s,[44] metallopharmaceuticals based on this element have long been overshadowed by their platinum counterparts, most notably cisplatin and its derivatives,[45] as anticancer therapeutic agents.[46] This was due in part to their poor solubility and stability in water. Since the mid-1990s, however, ruthenium−arene species have emerged as robust, highly active, and selective antitumoral and antimetastatic drugs toward various lines of cancerous cells, both *in vitro* and *in vivo*.[47] Accordingly, tremendous research efforts have been devoted to the synthesis and biological evaluation of neutral [$RuCl_2$(*p*-cymene)(L)] or cationic [RuCl(*p*-cymene)(L−L′)]X complexes bearing carefully designed mono- (L) or bidentate ligands (L−L′) to ensure a good water compatibility and a high activity.[48] Moreover, the critical influence of the counteranion was also highlighted in several reports.[49]

To the best of our knowledge, the biological activity of ruthenium−arene complexes bearing imidazol(in)ium-2-dithiocarboxylate ligands had never been investigated so far. Hence, we decided to probe the antitumoral activity and the cytotoxicity of [RuCl(*p*-cymene)(S_2C·NHC)]Cl complexes **2a**−**e** toward K562 human erythroleukemic cells and mouse splenocytes, respectively. We reasoned that the monometallic complexes would be more suitable for this exploratory work than the bimetallic salts **3a**−**e** because they have a well-defined structure with a single type of ruthenium centers. Besides, NMR spectroscopy showed that the [$RuCl_3$(*p*-cymene)]$^-$ anion was not observed in DMSO and water (*vide supra*), the two solvents used for the cell viability tests. Very gratifyingly, all five monometallic compounds were biologically active already at micromolar concentrations (Table 8). With a half maximal inhibitory concentration (IC_{50}) for K562 erythroleukemic cells of 0.05 μM and a cytotoxic concentration (CC_{50}) for mouse splenocytes of 0.07 μM, the [RuCl(*p*-cymene)(S_2C·IMes)]Cl complex **2a** displayed the highest *in vitro* toxicity toward both the cancerous and healthy cells. It was also slightly selective toward the former ones. Contrast-

https://doi.org/10.1021/acs.inorgchem.1c02648
Inorg. Chem. 2021, 60, 16769−16781

Table 8. Half Maximal Inhibitory Concentration (IC_{50}) for K562 Erythroleukemic Cells, Cytotoxic Concentration (CC_{50}) for Mouse Splenocytes, and Selectivity Index (SI) for the [RuCl(*p*-cymene)(S_2C·NHC)]Cl Complexes (2a−e)

complex (NHC)	IC_{50} (μM)[a]	CC_{50} (μM)[a]	SI[b]
2a (IMes)	0.051 ± 0.021 (3)	0.068 ± 0.022 (3)	1.33
2b (IDip)	0.308 ± 0.121 (3)	0.213 ± 0.139 (3)	0.69
2c (ICy)	5.808 ± 1.627 (4)	3.075 ± 0.179 (2)	0.53
2d (SIMes)	1.014 ± 0.426 (4)	1.713 ± 0.624 (2)	1.69
2e (SIDip)	0.139 ± 0.004 (2)	4.489 ± 0.388 (2)	32.1

[a]Numbers of independent experiments are given in parentheses. [b]SI = CC_{50}/IC_{50}.

ingly, complex **2c** bearing cycloalkyl groups on the nitrogen atoms of its imidazolium ring was the least active cytotoxic agent of our screening, and its selectivity was unfavorably reversed. Complex **2e** featuring the SIDip·CS_2 ligand emerged as the most promising candidate for further biological investigations, as it exhibited a high cytotoxicity remarkably targeted against the tumor cell line.

In a final series of experiments, we assessed the antitumoral activity of bimetallic complexes **3a−e** toward the K562 erythroleukemic cells. As discussed above (*cf.* Figure 5), aquation and solvation reactions are expected to occur in buffered culture media containing DMSO and water.[25,26] At this point, however, the actual species present in solution remain unknown. It should be kept in mind, also, that a double dose of ruthenium is available from the association of an [RuCl(*p*-cymene)(S_2C·NHC)]$^+$ cation with the [$RuCl_3$(*p*-cymene)]$^-$ anion. Nonetheless, when starting from bimetallic salts **3b**, **3d**, or **3e**, we obtained lower IC_{50} values than those recorded for the corresponding monometallic complexes **2b**, **2d**, and **2e** (Table 9). The opposite trend was observed when comparing the **2a**/**3a** and **2c**/**3c** pairs. Thus, no clear-cut tendency could be deduced to predict the influence of the anionic counterion.

Table 9. Half Maximal Inhibitory Concentration (IC_{50}) for K562 Erythroleukemic Cells of the Monometallic [RuCl(*p*-cymene)(S_2C·NHC)]Cl Complexes (2a−e) and the Bimetallic [RuCl(*p*-cymene)(S_2C·NHC)][$RuCl_3$(*p*-cymene)] Complexes (3a−e)

complex	IC_{50} (μM)[a]	complex	IC_{50} (μM)[a]
2a	0.051 ± 0.021 (3)	**3a**	0.485 ± 0.254 (4)
2b	0.308 ± 0.121 (3)	**3b**	0.151 ± 0.130 (3)
2c	5.808 ± 1.627 (4)	**3c**	7.102 ± 0.043 (1)
2d	1.014 ± 0.426 (4)	**3d**	0.559 ± 0.319 (2)
2e	0.139 ± 0.004 (2)	**3e**	0.095 ± 0.046 (3)

[a]Numbers of independent experiments are given in parentheses.

CONCLUSION AND PERSPECTIVES

An efficient synthetic protocol was devised for the preparation of five cationic ruthenium−arene complexes bearing imidazol(in)ium-2-dithiocarboxylate ligands from the [$RuCl_2$(*p*-cymene)]$_2$ dimer and *2 equiv* of an NHC·CS_2 zwitterion. When the metal source was reacted with only *1 equiv* of a dithiolate betaine, a set of five bimetallic salts with the generic formula [RuCl(*p*-cymene)(S_2C·NHC)][$RuCl_3$(*p*-cymene)] was obtained in quantitative yields. These novel, dual anionic and cationic ruthenium−arene complexes were fully characterized by various analytical techniques, and the molecular structures of two monometallic and two bimetallic complexes were solved by X-ray diffraction analysis.

NMR titrations showed that the chelation of the dithiocarboxylate ligands to afford cationic ruthenium−arene complexes was quantitative and irreversible. Conversely, the formation of the trichlorido(*p*-cymene)ruthenate anion was limited by an equilibrium, and this species readily dissociated into chloride anions and the [$RuCl_2$(*p*-cymene)]$_2$ dimer. The position of the equilibrium was strongly influenced by the nature of the solvent and was rather insensitive to the temperature. At 25 °C in $CDCl_3$, the dissociation constant of [$RuCl_3$(*p*-cymene)]$^-$ was K_d = 0.02 mol L^{-1}.

Samples subjected to XRD analysis after recrystallization of compounds **3a−e** in water/organic solvent mixtures contained either mono- or bimetallic complexes cocrystallized with H_2O. The presence of [$RuCl_2$(*p*-cymene)]$_2$ was also evidenced in the crystal phase, thereby confirming the reversible dissociation of the [$RuCl_3$(*p*-cymene)]$^-$ anion. Furthermore, crystallography highlighted the existence of strong interactions between the azolium ring protons of the [RuCl(*p*-cymene)(S_2C·NHC)]$^+$ cations and neighboring *n*- or π-donor groups in the solid state. These hydrogen bonds are most likely responsible for the large differences of chemical shifts evidenced by ^{1}H NMR spectroscopy when monitoring the resonances of the azolium backbone protons in solution. The facile cocrystallization of compounds **3a−e** with water prompted us to determine their aqueous solubility. A 0.01 M saturation concentration was reached with the [RuCl(*p*-cymene)(S_2C·IMes)][$RuCl_3$(*p*-cymene)] complex (**3a**) at room temperature. This corresponds to a 0.02 M concentration in metal species.

The *in vitro* antiproliferative activity of monometallic complexes **2a−e** and bimetallic salts **3a−e** was evaluated on K562 human leukemia cells. All the compounds tested were highly cytotoxic against these tumorous cells (IC_{50} = 0.05−7.10 μM). Furthermore, the SIDip-based complex **2e** displayed a remarkable selectivity toward cancerous vs normal cells.

Altogether, this study allowed us to better understand the equilibrium that governs the formation of the [$RuCl_3$(*p*-cymene)]$^-$ anion and to devise an efficient synthetic protocol for the synthesis of dual anionic and cationic ruthenium−arene complexes. Bimetallic compounds of this type had seldom been described in the literature and were isolated fortuitously in most cases. We showed that the use of zwitterionic ligands that form strong hydrogen bonds through their positively charged azolium ring and the recourse to a ruthenate complex instead of the more common halide counterions were two factors contributing to a high solubility of ruthenium−arene species in water. We also uncovered that mono- and bimetallic ruthenium−arene complexes bearing imidazol(in)ium-2-dithiocarboxylate ligands were highly active and selective cytotoxic agents. Further investigations to better appraise the potentials of these compounds as metallodrugs are underway and will be reported in due course.

ASSOCIATED CONTENT

Supporting Information

The Supporting Information is available free of charge at https://pubs.acs.org/doi/10.1021/acs.inorgchem.1c02648.

Experimental procedures and analytical data for compounds **2a−e** and **3a−e** (PDF)

https://doi.org/10.1021/acs.inorgchem.1c02648
Inorg. Chem. 2021, 60, 16769−16781

Computational details for determination of K_d (XLS)

Accession Codes

CCDC 2037518−2037521 contain the supplementary crystallographic data for this paper. These data can be obtained free of charge via www.ccdc.cam.ac.uk/data_request/cif, or by emailing data_request@ccdc.cam.ac.uk, or by contacting The Cambridge Crystallographic Data Centre, 12 Union Road, Cambridge CB2 1EZ, UK; fax: +44 1223 336033.

AUTHOR INFORMATION

Corresponding Author

Lionel Delaude − *Laboratory of Catalysis, MolSys Research Unit, Institut de Chimie Organique (B6a), Université de Liège, 4000 Liège, Belgium;* orcid.org/0000-0002-1134-2992; Email: l.delaude@uliege.be

Authors

Mohammed Zain Aldin − *Laboratory of Catalysis, MolSys Research Unit, Institut de Chimie Organique (B6a), Université de Liège, 4000 Liège, Belgium*

Guillermo Zaragoza − *Unidade de Difracción de Raios X, RIAIDT, Universidade de Santiago de Compostela, 15782 Santiago de Compostela, Spain;* orcid.org/0000-0002-2550-6628

William Deschamps − *Department of Molecular Biology, Institute for Molecular Biology and Medicine, Université Libre de Bruxelles, 6041 Gosselies, Belgium*

Jean-Claude Didelot Tomani − *Department of Molecular Biology, Institute for Molecular Biology and Medicine, Université Libre de Bruxelles, 6041 Gosselies, Belgium*

Jacob Souopgui − *Department of Molecular Biology, Institute for Molecular Biology and Medicine, Université Libre de Bruxelles, 6041 Gosselies, Belgium*

Complete contact information is available at: https://pubs.acs.org/10.1021/acs.inorgchem.1c02648

Notes

The authors declare no competing financial interest.

ACKNOWLEDGMENTS

Financial support from the Fonds de la Recherche Scientifique - FNRS under Grant CDR J.0155.18 is gratefully acknowledged. The authors would like to thank Dr. Nicolas Smargiasso for the ESI-MS analyses, Mr. Stéphane Luts and Prof. Gauthier Eppe for the FT-IR analyses, and RIAIDT-USC for the use of its analytical facilities.

REFERENCES

(1) (a) Kuhn, N.; Bohnen, H.; Henkel, G. About the Reaction of Carbon Disulfide Carbene Adducts with Bromine and Iodine. *Z. Naturforsch., B: J. Chem. Sci.* **1994**, *49*, 1473−1480. (b) Enders, D.; Breuer, K.; Runsink, J.; Teles, J. H. Chemical reactions of the stable carbene 1,3,4-triphenyl-4,5-dihydro-1H-1,2,4-triazol-5-ylidene. *Liebigs Ann. Chem.* **1996**, *1996*, 2019−2028. (c) Kuhn, N.; Niquet, E.; Steimann, M.; Walker, I. Methoxyalkyl-functionalized 2,3-dihydroimidazol-2-ylidenes. *Z. Naturforsch., B: J. Chem. Sci.* **1999**, *54*, 1181−1187. (d) Sereda, O.; Blanrue, A.; Wilhelm, R. Enantiopure imidazolinium-dithiocarboxylates as highly selective novel organocatalysts. *Chem. Commun.* **2009**, 1040−1042. (e) Dagmara Konieczna, D.; Blanrue, A.; Wilhelm, R. Investigation of Imidazol(in)ium-dithiocarboxylates as Sensors for the Detection of Mercury(II) and Silver(I) Ions. *Z. Naturforsch., B: J. Chem. Sci.* **2014**, *69*, 596.

(2) Delaude, L.; Demonceau, A.; Wouters, J. Assessing the Potentials of Zwitterionic NHC·CS_2 Adducts for Probing the Stereoelectronic Parameters of N-Heterocyclic Carbenes. *Eur. J. Inorg. Chem.* **2009**, 1882−1891.

(3) (a) Delaude, L. Betaine Adducts of N-Heterocyclic Carbenes: Synthesis, Properties, and Reactivity. *Eur. J. Inorg. Chem.* **2009**, 1681−1699. (b) Beltrán, T. F.; Delaude, L. Recent Advances in Small Clusters and Polymetallic Assemblies Based on Transition Metals and Dithiocarboxylate Zwitterions Derived from N-Heterocyclic Carbenes. *J. Cluster Sci.* **2017**, *28*, 667−678.

(4) (a) Borer, L. L.; Kong, J. V. Octahedral nickel(II) dithiocarboxylates. *Inorg. Chim. Acta* **1986**, *122*, 145−148. (b) Borer, L. L.; Kong, J. V.; Keihl, P. A.; Forkey, D. M. Metal complexes of 1,3-dimethylimidazolium-2-dithiocarboxylate. *Inorg. Chim. Acta* **1987**, *129*, 223−226.

(5) Delaude, L.; Sauvage, X.; Demonceau, A.; Wouters, J. Synthesis and Catalytic Evaluation of Ruthenium-Arene Complexes Generated Using Imidazol(in)ium-2-carboxylates and -Dithiocarboxylates. *Organometallics* **2009**, *28*, 4056−4064.

(6) Naeem, S.; Thompson, A. L.; Delaude, L.; Wilton-Ely, J. D. E. T. Non-innocent Behaviour of Dithiocarboxylate Ligands Based on N-Heterocyclic Carbenes. *Chem. - Eur. J.* **2010**, *16*, 10971−10974.

(7) Naeem, S.; Thompson, A. L.; White, A. J. P.; Delaude, L.; Wilton-Ely, J. D. E. T. Dithiocarboxylate Complexes of Ruthenium(II) and Osmium(II). *Dalton Trans.* **2011**, *40*, 3737−3747.

(8) Champion, M. J. D.; Solanki, R.; Delaude, L.; White, A. J. P.; Wilton-Ely, J. D. E. T. Synthesis and Catalytic Application of Palladium Imidazol(in)ium-2-dithiocarboxylate Complexes. *Dalton Trans.* **2012**, *41*, 12386−12394.

(9) Naeem, S.; Delaude, L.; White, A. J. P.; Wilton-Ely, J. D. E. T. The Use of Imidazolium-2-dithiocarboxylates in the Formation of Gold(I) Complexes and Gold Nanoparticles. *Inorg. Chem.* **2010**, *49*, 1784−1793.

(10) Beltrán, T. F.; Zaragoza, G.; Delaude, L. Mono- and bimetallic manganese-carbonyl complexes and clusters bearing imidazol(in)ium-2-dithiocarboxylate ligands. *Dalton Trans.* **2017**, *46*, 1779−1788.

(11) Beltrán, T. F.; Zaragoza, G.; Delaude, L. Synthesis, characterization, and gas-phase fragmentation of rhenium-carbonyl complexes bearing imidazol(in)ium-2-dithiocarboxylate ligands. *Dalton Trans.* **2016**, *45*, 18346−18355.

(12) See also: Zhao, J.; Sun, H.; Liu, L.; Chang, W.; Li, J. Synthesis, Characterization and Potential Electrochemical Properties of Novel Mn-Re Dinuclear Complexes Containing N-Heterocyclic Carbene-Carbon Disulfide Ligands. *Chem. J. Chin. Univ.* **2014**, *35*, 68−74.

(13) Beltrán, T. F.; Zaragoza, G.; Delaude, L. Synthesis and complexation of superbulky imidazolium-2-dithiocarboxylate ligands. *Dalton Trans.* **2017**, *46*, 9036−9048.

(14) Neuba, A.; Ortmeyer, J.; Konieczna, D. D.; Weigel, G.; Flörke, U.; Henkel, G.; Wilhelm, R. Synthesis of New Copper(I) Based Linear 1-D-Coordination Polymers with Neutral Imidazolinium-dithiocarboxylate Ligands. *RSC Adv.* **2015**, *5*, 9217−9220.

(15) Ortmeyer, J.; Flörke, U.; Wilhelm, R.; Henkel, G.; Neuba, A. A Sophisticated Approach towards a New Class of Copper(I) Sulfur Cluster Complexes with Imidazolinium-dithiocarboxylate Ligands. *Eur. J. Inorg. Chem.* **2017**, 3191−3197.

(16) Siemeling, U.; Memczak, H.; Bruhn, C.; Vogel, F.; Trager, F.; Baio, J. E.; Weidner, T. Zwitterionic Dithiocarboxylates Derived from N-Heterocyclic Carbenes: Coordination to Gold Surfaces. *Dalton Trans.* **2012**, *41*, 2986−2994.

(17) (a) Shi, Y.-C.; Shi, Y. Synthesis, Crystal Structure and Electrochemical Study of (μ-κ^2C:κ^2S-NHC$^+$-CS)[$Fe_2(CO)_6$]$^-$ Generated from the Reaction of NHC$^+$-CS_2^- with $Fe_3(CO)_{12}$. *Inorg. Chim. Acta* **2015**, *434*, 92−96. (b) Beltrán, T. F.; Zaragoza, G.; Delaude, L. Small iron-carbonyl clusters bearing imidazolium-2-trithioperoxycarboxylate ligands. *Dalton Trans.* **2017**, *46*, 13002−13009.

(18) Cabeza, J. A.; García-Álvarez, P.; Hernández-Cruz, M. G. Reactions of CS_2 and C(S)NPh Adducts of N-Heterocyclic Carbenes with [$Ru_3(CO)_{12}$]: Remarkable Reactivity of These Betaines

Involving One or Two C-S Bond Activation Processes. *Eur. J. Inorg. Chem.* **2012**, 2928−2932.
(19) (a) Delaude, L.; Demonceau, A. Retracing the evolution of monometallic ruthenium-arene catalysts for C-C bond formation. *Dalton Trans.* **2012**, *41*, 9257−9268. (b) Méret, M.; Maj, A. M.; Demonceau, A.; Delaude, L. Ruthenium-arene catalysts bearing N-heterocyclic carbene ligands for olefin cyclopropanation and metathesis. *Monatsh. Chem.* **2015**, *146*, 1099−1105.
(20) Sun, Y.; Machala, M. L.; Castellano, F. N. Controlled microwave synthesis of Ru^{II} synthons and chromophores relevant to solar energy conversion. *Inorg. Chim. Acta* **2010**, *363*, 283−287.
(21) Vock, C. A.; Dyson, P. J. Improved synthesis of the [Ru(η^6-*p*-cymene)Cl_3] anion: facile isolation under mild conditions. *Z. Anorg. Allg. Chem.* **2007**, *633*, 640−642.
(22) (a) Robertson, D. R.; Stephenson, T. A. Cationic and anionic complexes of ruthenium(II) containing η^6-arene ligands. *J. Organomet. Chem.* **1976**, *116*, C29−C30. (b) Robertson, D. R.; Stephenson, T. A.; Arthur, T. Cationic, Neutral and Anionic Complexes of Ruthenium-(II) containing η^6-Arene Ligands. *J. Organomet. Chem.* **1978**, *162*, 121−136.
(23) (a) Zelonka, R. A.; Baird, M. C. Benzene Complexes of Ruthenium(II). *Can. J. Chem.* **1972**, *50*, 3063−3072. (b) Bennett, M. A.; Smith, A. K. Arene ruthenium(II) complexes formed by dehydrogenation of cyclohexadienes with ruthenium(III) trichloride. *J. Chem. Soc., Dalton Trans.* **1974**, 233−241. (c) Gould, R. O.; Jones, C. L.; Robertson, D. R.; Stephenson, T. A. Preparation, X-ray crystal structure analysis, and reactions of a novel, hydroxo-bridged, tetranuclear, π-arene ruthenium(II) quadrivalent cation [{(η^6-C_6H_6)-Ru(OH)}$_4$]$(SO_4)_2$·$12H_2O$. *J. Chem. Soc., Chem. Commun.* **1977**, 222−223. (d) Hung, Y.; Kung, W.-J.; Taube, H. Aquo chemistry of monoarene complexes of osmium(II) and ruthenium(II). *Inorg. Chem.* **1981**, *20*, 457−463. (e) Stebler-Röthlisberger, M.; Hummel, W.; Pittet, P. A.; Bürgi, H. B.; Ludi, A.; Merbach, A. E. Triaqua(benzene)-ruthenium(II) and triaqua(benzene)osmium(II): synthesis, molecular structure, and water-exchange kinetics. *Inorg. Chem.* **1988**, *27*, 1358−1363.
(24) Süss-Fink, G. Water-soluble arene ruthenium complexes: From serendipity to catalysis and drug design. *J. Organomet. Chem.* **2014**, *751*, 2−19.
(25) Patra, M.; Joshi, T.; Pierroz, V.; Ingram, K.; Kaiser, M.; Ferrari, S.; Spingler, B.; Keiser, J.; Gasser, G. DMSO-Mediated Ligand Dissociation: Renaissance for Biological Activity of N-Heterocyclic-[Ru(η^6-arene)Cl_2] Drug Candidates. *Chem. - Eur. J.* **2013**, *19*, 14768−14772.
(26) (a) Wang, F.; Chen, H.; Parsons, S.; Oswald, I. D. H.; Davidson, J. E.; Sadler, P. J. Kinetics of Aquation and Anation of Ruthenium(II) Arene Anticancer Complexes, Acidity and X-ray Structures of Aqua Adducts. *Chem. - Eur. J.* **2003**, *9*, 5810−5820. (b) Wang, F.; Habtemariam, A.; van der Geer, E. P. L.; Fernández, R.; Melchart, M.; Deeth, R. J.; Aird, R.; Guichard, S.; Fabbiani, F. P. A.; Lozano-Casal, P.; Oswald, I. D. H.; Jodrell, D. I.; Parsons, S.; Sadler, P. J. Controlling ligand substitution reactions of organometallic complexes: Tuning cancer cell cytotoxicity. *Proc. Natl. Acad. Sci. U. S. A.* **2005**, *102*, 18269. (c) Ang, W. H.; Daldini, E.; Scolaro, C.; Scopelliti, R.; Juillerat-Jeannerat, L.; Dyson, P. J. Development of Organometallic Ruthenium-Arene Anticancer Drugs That Resist Hydrolysis. *Inorg. Chem.* **2006**, *45*, 9006−9013. (d) Scolaro, C.; Hartinger, C. G.; Allardyce, C. S.; Keppler, B. K.; Dyson, P. J. Hydrolysis study of the bifunctional antitumour compound RAPTA-C, [Ru(η^6-*p*-cymene)Cl_2(pta)]. *J. Inorg. Biochem.* **2008**, *102*, 1743−1748. (e) Futera, Z.; Klenko, J.; Šponer, J. E.; Šponer, J.; Burda, J. V. Interactions of the "piano-stool" [ruthenium(II)(η^6-arene)(en)Cl]$^+$ complexes with water and nucleobases; ab initio and DFT study. *J. Comput. Chem.* **2009**, *30*, 1758−1770. (f) Zhao, J.; Zhang, X.; Liu, H.; Xiong, Z.; Li, M.; Chen, T. Ruthenium arene complex induces cell cycle arrest and apoptosis through activation of P53-mediated signaling pathways. *J. Organomet. Chem.* **2019**, *898*, 120869.
(27) Cabeza, J. A.; da Silva, I.; del Rio, I.; Garcia-Granda, S. [*N*,*N*′-Bis-(6-methylpyrid-2-ylium)-(1*R*,2*R*)-1,2-diaminocyclohexane] bis-[(*p*-cymene)-trichlororuthenate(II)]. *Appl. Organomet. Chem.* **2005**, *19*, 209−210.
(28) Arslan, H.; Van der Veer, D.; Özdemir, I.; Gürbüz, N.; Gök, Y.; Çetinkaya, B. 1,3-Bis(thiophen-2-ylmethyl)-3,4,5,6-tetrahydropyrimidinium trichlorido(η^6-*p*-cymene)ruthenate(II). *Acta Crystallogr., Sect. E: Struct. Rep. Online* **2009**, *65*, m111−m112.
(29) (a) Arslan, H.; Van der Veer, D.; Özdemir, I.; Gürbüz, N.; Gök, Y.; Çetinkaya, B. 1,3-Bis(2-thienylmethyl)-4,5-dihydroimidazolium trichlorido(η^6-*p*-cymene)ruthenate(II). *Acta Crystallogr., Sect. E: Struct. Rep. Online* **2009**, *65*, m165−m166. (b) Ibáñez, S.; Poyatos, M.; Peris, E. A D_{3h}-symmetry hexaazatriphenylene-tris-N-heterocyclic carbene ligand and its coordination to iridium and gold: preliminary catalytic studies. *Chem. Commun.* **2017**, *53*, 3733−3736.
(30) Wu, F. H.; Lu, L.; Duan, T.; Zhang, Q. F. Tetraethylammonium trichlorido(η^6-*p*-cymene)ruthenate(II). *Acta Crystallogr., Sect. E: Struct. Rep. Online* **2009**, *65*, No. m1695.
(31) Krstić, M.; Sovilj, S. P.; Grgurić-Šipka, S.; Evans, I. R.; Borozan, S.; Santibanez, J. F. Synthesis, structural and spectroscopic characterization, *in vitro* cytotoxicity and *in vivo* activity as free radical scavengers of chlorido(*p*-cymene) complexes of ruthenium(II) containing N-alkylphenothiazines. *Eur. J. Med. Chem.* **2011**, *46*, 4168−4177.
(32) (a) Toennemann, J.; Scopelliti, R.; Severin, K. (Arene) ruthenium Complexes with Imidazolin-2-imine and Imidazolidin-2-imine Ligands. *Eur. J. Inorg. Chem.* **2014**, 4287−4293. (b) Kishan, R.; Kumar, R.; Baskaran, S.; Sivasankar, C.; Thirupathi, N. Ionic and Neutral Half-Sandwich Guanidinatoruthenium(II) Complexes and Their Solution Behavior. *Eur. J. Inorg. Chem.* **2015**, 3182−3194.
(33) Vock, C. A.; Scolaro, C.; Phillips, A. D.; Scopelliti, R.; Sava, G.; Dyson, P. J. Synthesis, Characterization, and in Vitro Evaluation of Novel Ruthenium(II) η^6-Arene Imidazole Complexes. *J. Med. Chem.* **2006**, *49*, 5552−5561.
(34) Marchetti, F.; Pettinari, C.; Pettinari, R.; Cerquetella, A.; Di Nicola, C.; Macchioni, A.; Zuccaccia, D.; Monari, M.; Piccinelli, F. Synthesis and Intramolecular and Interionic Structural Characterization of Half-Sandwich (Arene)Ruthenium(II) Derivatives of Bis(Pyrazolyl)Alkanes. *Inorg. Chem.* **2008**, *47*, 11593−11603.
(35) Zhou, Q.; Li, P.; Lu, R.; Qian, Q.; Lei, X.; Xiao, Q.; Huang, S.; Liu, L.; Huang, C.; Su, W. Synthesis, X-ray Diffraction Study, and Cytotoxicity of a Cationic *p*-Cymene Ruthenium Chloro Complex Containing a Chelating Semicarbazone Ligand. *Z. Anorg. Allg. Chem.* **2013**, *639*, 943−946.
(36) Su, W.; Tang, Z.; Xiao, Q.; Li, P.; Qian, Q.; Lei, X.; Huang, S.; Peng, B.; Cui, J.; Huang, C. Synthesis, structures, antiproliferative activity of a series of ruthenium(II) arene derivatives of thiosemicarbazones ligands. *J. Organomet. Chem.* **2015**, *783*, 10−16.
(37) Mu, C.; Prosser, K. E.; Harrypersad, S.; MacNeil, G. A.; Panchmatia, R.; Thompson, J. R.; Sinha, S.; Warren, J. J.; Walsby, C. J. Activation by Oxidation: Ferrocene-Functionalized Ru(II)-Arene Complexes with Anticancer, Antibacterial, and Antioxidant Properties. *Inorg. Chem.* **2018**, *57*, 15247−15261.
(38) Volbeda, J.; Jones, P. G.; Tamm, M. Preparation of chiral imidazolin-2-imine ligands and their application in ruthenium-catalyzed transfer hydrogenation. *Inorg. Chim. Acta* **2014**, *422*, 158−166.
(39) Mayfield, H. G.; Bull, W. E. Co-ordinating tendencies of the hexafluorophosphate ion. *J. Chem. Soc. A* **1971**, 2279−2281.
(40) (a) Therrien, B. Functionalised η^6-arene ruthenium complexes. *Coord. Chem. Rev.* **2009**, *253*, 493−519. (b) Kumar, P.; Gupta, R. K.; Pandey, D. S. Half-sandwich arene ruthenium complexes: synthetic strategies and relevance in catalysis. *Chem. Soc. Rev.* **2014**, *43*, 707−733. (c) Singh, A. K.; Pandey, D. S.; Xu, Q.; Braunstein, P. Recent advances in supramolecular and biological aspects of arene ruthenium(II) complexes. *Coord. Chem. Rev.* **2014**, *270*−*271*, 31−56.
(41) Allen, F. H.; Watson, D. G.; Brammer, L.; Orpen, A. G.; Taylor, R. In *International Tables for Crystallography*; Prince, E., Ed.; Springer: Berlin, 2006; Vol. *C*, pp 790−811.
(42) Martínez-Alonso, M.; Sanz, P.; Ortega, P.; Espino, G.; Jalón, F. A.; Martín, M.; Rodríguez, A. M.; López, J. A.; Tejel, C.; Manzano, B.

https://doi.org/10.1021/acs.inorgchem.1c02648
Inorg. Chem. 2021, 60, 16769−16781

R. Analysis of Ion Pairing in Solid State and Solution in *p*-Cymene Ruthenium Complexes. *Inorg. Chem.* **2020**, *59*, 14171−14183.
(43) See for instance: (a) Martínez-Alonso, M.; Busto, N.; Jalón, F. A.; Manzano, B. R.; Leal, J. M.; Rodríguez, A. M.; García, B.; Espino, G. Derivation of Structure-Activity Relationships from the Anticancer Properties of Ruthenium(II) Arene Complexes with 2-Aryldiazole Ligands. *Inorg. Chem.* **2014**, *53*, 11274−11288. (b) Kumar, A.; Kumar, A.; Gupta, R. K.; Paitandi, R. P.; Singh, K. B.; Trigun, S. K.; Hundal, M. S.; Pandey, D. S. Cationic Ru(II), Rh(III) and Ir(III) complexes containing cyclic π-perimeter and 2-aminophenyl benzimidazole ligands: Synthesis, molecular structure, DNA and protein binding, cytotoxicity and anticancer activity. *J. Organomet. Chem.* **2016**, *801*, 68−79. (c) Guerriero, A.; Oberhauser, W.; Riedel, T.; Peruzzini, M.; Dyson, P. J.; Gonsalvi, L. New Class of Half-Sandwich Ruthenium(II) Arene Complexes Bearing the Water-Soluble CAP Ligand as an in Vitro Anticancer Agent. *Inorg. Chem.* **2017**, *56*, 5514−5518. (d) Haribabu, J.; Srividya, S.; Umapathi, R.; Gayathri, D.; Venkatesu, P.; Bhuvanesh, N.; Karvembu, R. Enhanced anticancer activity of half-sandwich Ru(II)-*p*-cymene complex bearing heterocyclic hydrazone ligand. *Inorg. Chem. Commun.* **2020**, *119*, 108054.
(44) Dwyer, F. P.; Gyarfas, E. C.; Rogers, W. P.; Koch, J. H. Biological Activity of Complex Ions. *Nature* **1952**, *170*, 190−191.
(45) (a) Alderden, R. A.; Hall, M. D.; Hambley, T. W. The Discovery and Development of Cisplatin. *J. Chem. Educ.* **2006**, *83*, 728−734. (b) Ghosh, S. Cisplatin: The first metal based anticancer drug. *Bioorg. Chem.* **2019**, *88*, 102925.
(46) Thota, S.; Rodrigues, D. A.; Crans, D. C.; Barreiro, E. J. Ru(II) Compounds: Next-Generation Anticancer Metallotherapeutics? *J. Med. Chem.* **2018**, *61*, 5805−5821.
(47) (a) Süss-Fink, G. Arene ruthenium complexes as anticancer agents. *Dalton Trans.* **2010**, *39*, 1673−1688. (b) Ang, W. H.; Casini, A.; Sava, G.; Dyson, P. J. Organometallic ruthenium-based antitumor compounds with novel modes of action. *J. Organomet. Chem.* **2011**, *696*, 989−998. (c) Noffke, A. L.; Habtemariam, A.; Pizarro, A. M.; Sadler, P. J. Designing organometallic compounds for catalysis and therapy. *Chem. Commun.* **2012**, *48*, 5219−5246. (d) Nazarov, A. A.; Hartinger, C. G.; Dyson, P. J. Opening the lid on piano-stool complexes: An account of ruthenium(II)-arene complexes with medicinal applications. *J. Organomet. Chem.* **2014**, *751*, 251−260. (e) Singh, S. K.; Pandey, D. S. Multifaceted half-sandwich arene-ruthenium complexes: interactions with biomolecules, photoactivation, and multinuclearity approach. *RSC Adv.* **2014**, *4*, 1819−1840. (f) Blunden, B. M.; Stenzel, M. H. Incorporating ruthenium into advanced drug delivery carriers - an innovative generation of chemotherapeutics. *J. Chem. Technol. Biotechnol.* **2015**, *90*, 1177−1195. (g) Mari, C.; Pierroz, V.; Ferrari, S.; Gasser, G. Combination of Ru(II) complexes and light: new frontiers in cancer therapy. *Chem. Sci.* **2015**, *6*, 2660−2686. (h) Murray, B. S.; Babak, M. V.; Hartinger, C. G.; Dyson, P. J. The development of RAPTA compounds for the treatment of tumors. *Coord. Chem. Rev.* **2016**, *306*, 86−114.
(48) For a few recent examples, see: (a) Montani, M.; Pazmay, G. V. B.; Hysi, A.; Lupidi, G.; Pettinari, R.; Gambini, V.; Tilio, M.; Marchetti, F.; Pettinari, C.; Ferraro, S.; Iezzi, M.; Marchini, C.; Amici, A. The water soluble ruthenium(II) organometallic compound [Ru(*p*-cymene)(bis(3,5-dimethylpyrazol-1-yl)methane)Cl]Cl suppresses triple negative breast cancer growth by inhibiting tumor infiltration of regulatory T cells. *Pharmacol. Res.* **2016**, *107*, 282−290. (b) Marchetti, F.; Pettinari, R.; Di Nicola, C.; Pettinari, C.; Palmucci, J.; Scopelliti, R.; Riedel, T.; Therrien, B.; Galindo, A.; Dyson, P. J. Synthesis, characterization and cytotoxicity of arene-ruthenium(II) complexes with acylpyrazolones functionalized with aromatic groups in the acyl moiety. *Dalton Trans.* **2018**, *47*, 868−878. (c) Swaminathan, S.; Haribabu, J.; Kalagatur, N. K.; Konakanchi, R.; Balakrishnan, N.; Bhuvanesh, N.; Karvembu, R. Synthesis and Anticancer Activity of $[RuCl_2(\eta^6\text{-arene})(\text{aroylthiourea})]$ Complexes—High Activity against the Human Neuroblastoma (IMR-32) Cancer Cell Line. *ACS Omega* **2019**, *4*, 6245−6256. (d) Khan, T. A.; Bhar, K.; Thirumoorthi, R.; Roy, T. K.; Sharma, A. K. Design, synthesis, characterization and evaluation of the anticancer activity of water-soluble half-sandwich ruthenium(II) arene halido complexes. *New J. Chem.* **2020**, *44*, 239−257. (e) Chen, C.; Xu, C.; Li, T.; Lu, S.; Luo, F.; Wang, H. Novel NHC-coordinated ruthenium(II) arene complexes achieve synergistic efficacy as safe and effective anticancer therapeutics. *Eur. J. Med. Chem.* **2020**, *203*, 112605.
(49) (a) Loughrey, B. T.; Healy, P. C.; Parsons, P. G.; Williams, M. L. Selective Cytotoxic Ru(II) Arene Cp* Complex Salts [R-PhRuCp*]$^+X^-$ for X = BF_4^-, PF_6^-, and BPh_4^-. *Inorg. Chem.* **2008**, *47*, 8589−8591. (b) Magut, P. K. S.; Das, S.; Fernand, V. E.; Losso, J.; McDonough, K.; Naylor, B. M.; Aggarwal, S.; Warner, I. M. Tunable Cytotoxicity of Rhodamine 6G via Anion Variations. *J. Am. Chem. Soc.* **2013**, *135*, 15873−15879. (c) Haghdoost, M. M.; Golbaghi, G.; Guard, J.; Sielanczyk, S.; Patten, S. A.; Castonguay, A. Synthesis, characterization and biological evaluation of cationic organoruthenium(II) fluorene complexes: influence of the nature of the counteranion. *Dalton Trans.* **2019**, *48*, 13396−13405.

https://doi.org/10.1021/acs.inorgchem.1c02648
Inorg. Chem. 2021, 60, 16769−16781